Sublimation-condensation phenomenon in microwave freeze-drying*, **

WANG Zhaohui (王朝晖) and SHI Mingheng (施明恒)

(Department of Power Engineering, Southeast University, Nanjing 210018, China)

Received December 23, 1997

Abstract A sublimation-condensation model is developed for microwave freeze-drying of unsaturated porous media. The transport properties in the model are analyzed and the model is calculated numerically for the microwave freeze-drying of unsaturated porous media. The results show that the effects of sublimation-condensation region on drying processes are significant as compared with the traditional sublimation interface model.

Keywords: freeze-drying, microwave heating, sublimation-condensation region, heat and mass transfer.

Freeze-drying is one of the key operations for the products of biology, pharmacology, food, and material. In order to increase the drying rate, decrease the drying time, and conserve energy, microwave freeze-drying is developed to overcome the disadvantages of conventional freeze-drying. During the freeze-drying process, water in the material occurs in solid phase and at the beginning of drying, the pores of the material may be filled with frozen water fully or partially, usually called saturated and unsaturated porous media respectively. The mechanism of heat and mass transfer is different for saturated and unsaturated porous media in freeze-drying, especially for microwave freeze-drying.

The reports about freeze-drying in literature were concentrated on saturated porous media and a comprehensive review was given by Arsem and Ma[1]. After the Luikov's theory of heat and mass transfer in porous media[2] was presented on the basis of irreversible thermodynamics, numerical simulation and analysis have become the hot point in the study of heat and mass transfer in freeze-drying[3—6]. However, all the above considers that sublimation takes place at a sublimation interface.

During the freeze-drying of unsaturated porous media, vapor will remove in frozen region due to the gradients of gas pressure and vapor concentration, and then ice sublimation or vapor condensation will appear in this region. The only study on freeze-drying of unsaturated porous media by Fey and Boles[7] analyzed the effects of vapor convection in frozen region on heat and mass

* Project supported by the National Natural Science Foundation of China.

** Nomenclature: c, specific heat capacity, J/(kg·℃); D, diffusivity, m^2/s; E, electric field strength, V/cm; f_J, contribution percentage of sublimation-condensation region to drying rate; f_m, moisture content fraction; f_T, coefficient of source conversion, kg/J; ΔH, latent heat of ice sublimation, J/kg; I, mass source intensity, kg/(m^3·s); J_F, mass flux caused by sublimation front, kg/(m^2·s); J_S, mass flux in sublimation-condensation region, kg/(m^2·s); J_v, mass flux in dried region, kg/(m^2·s); k, microwave dissipation coefficient, W/m^3·(V/cm)$^{-2}$; K_D, permeability of dried material, m^2; K_r, relative permeability; K_S, effective diffusivity, kg/(m·s·℃); l, calculating thickness (half sample thickness), m; P, gas pressure, Pa; q, internal heat source intensity, W/m^3; R, gas constant of vapor, m^2/(s^2·℃); S, saturation; T, temperature, K (or ℃); u_m, saturated moisture content, kg/m^3; x, space axis, m; X, sublimation front position, m; α, heat transfer coefficient, W/(m^2·℃); ε, porosity; λ, thermal conductivity, W/(m·℃); μ, viscosity, (kg·m)/s; ρ, density, kg/m^3; τ, time, s. Subscripts: 0, of initial value; D, in dried region; e, of effective value; i, of ice; R, of surrounding; s, of solid body; S, in sublimation-condensation region; v, of vapor; X, at sublimation front.

transfer in the drying process. Unfortunately, the saturation change caused by vapor movement is still not considered. As for freeze-drying with internal heat source, the reverse phenomenon will occur in the unsaturated frozen region with respect to that by surface heating. On the other hand, their results are limited by the constant assumption on the coefficients in Luikov's theory.

After using the volume average method, the theory of heat and mass transport for continuum media is introduced to porous media by Whitaker[8] and the drying model of heat and mass transfer is more available in practice. Here a mathematical model is developed for freeze-drying of unsaturated porous media on the basis of Whitaker's theory and the transport mechanism is analyzed. Also the model is calculated numerically for microwave freeze-drying of unsaturated porous media and the effect of sublimation-condensation region on drying processes is discussed.

1 Mathematical model

Under the vacuum condition of freeze-drying, three regions have been observed in the saturated frozen porous material, including the dried region, the sublimation region, and the frozen region. The sublimation region, where ice sublimation takes places, is so narrow as to be considered an infinitely thin area, called the sublimation interface, which separates the material into the frozen region and the dried region. Heat conduction is the only heat transfer mechanism in the frozen region while the vapor sublimated from the sublimation interface flows from the dried region. The sublimation interface model in literature is suggested on the above assumption.

During freeze-drying of unsaturated porous media, the dried region, sublimation interface, and frozen region will form just like the above case. The difference is that there exists vapor in the pores partially filled with frozen moisture. The vapor will be convected in the unsaturated frozen region under the gradients of gas pressure and vapor concentration. Then ice will be sublimated or vapor will be condensed in the frozen region, and the saturation in this region will consequently increase or decrease. In this study, such a frozen region is called the sublimation-condensation region and the previous sublimation interface is then called the sublimation front, by which the material is divided into the sublimation-condensation region and the dried region. The physical model for the freeze-drying of an unsaturated porous medium is illustrated in figure 1.

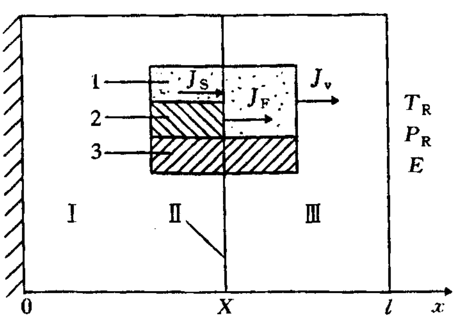

Fig. 1. Sublimation-condensation physical model. I, Sublimation-condensation region; II, sublimation front; III, dried region. 1, Vapor ($\varepsilon(1-S)$); 2, ice (εS); 3, solid body ($1-\varepsilon$).

In order to develop the heat and mass transfer equations, the following is assumed: (i) the solid body is rigid and no shrinkage exists; (ii) local thermodynamical equilibrium is available for the phases of porous media; (iii) the dissipation of gas flow is neglected; (iv) vapor is the only gas in vacuum chamber and can be considered as ideal gas; (v) the Darcy's law is available for vapor flow and the Fick's law is valid for vapor diffusion; (vi) the effect of absorbed water is neglected; (vii) the effect of salt on vapor pressure is not considered; (viii) the material is homogeneous and isotropic; (ix) the pores with gas phase are connected.

Considering the above assumptions, the heat and mass transfer equations for the sublimation-condensation region, dried region, and sublimation front will be developed respectively as follows.

1.1 Sublimation-condensation region

The vapor conservation equation can be described as

$$\frac{\partial}{\partial \tau}[(1-S)\varepsilon\rho_v] = -\frac{\partial J_S}{\partial x} + I. \tag{1}$$

If the heat transfer caused by vapor flow is neglected, the energy balance equation is

$$\rho c\frac{\partial T}{\partial \tau} = \frac{\partial}{\partial x}\left(\lambda\frac{\partial T}{\partial x}\right) - I\cdot\Delta H + q. \tag{2}$$

The vapor source can be determined as

$$I = -u_m\frac{\partial S}{\partial \tau}. \tag{3}$$

Based on Darcy's law and Fick's law, the vapor flux in sublimation-condensation region can be obtained:

$$J_S = -\frac{K_D K_r}{\mu_v}\rho_v\frac{\partial P}{\partial x} - (1-S)\varepsilon D\frac{\partial \rho_v}{\partial x}. \tag{4}$$

As to the saturated vapor of ideal gas, the above equation becomes

$$J_S = -K_S\frac{\partial T}{\partial x}, \tag{5}$$

where

$$K_S = \frac{K_D K_r}{\mu_v}R\rho_v^2 + \left[\frac{K_D K_r}{\mu_v}R\rho_v T + \varepsilon(1-S)D\right]\frac{d\rho_v}{dT}. \tag{6}$$

Equation (5) shows that the vapor flow direction depends on the temperature gradient. This means that the vapor will flow from the sublimation front to the sublimation-condensation region inside when the material is subjected to surface heating while from the material center to sublimation front when heated under internal heat generation. These two cases correspond to vapor condensation and ice sublimation respectively and the analysis by Fey and Boles[7] is just the former one.

Based on the fact that $\frac{\varepsilon\rho_v}{u_m} < \frac{\rho_v}{u_m} \ll 1$, the following can be obtained from eqs. (1), (3) and (5):

$$I = \varepsilon(1-S)\frac{d\rho_v}{dT}\cdot\frac{\partial T}{\partial \tau} - \frac{\partial}{\partial x}\left(K_S\frac{\partial T}{\partial x}\right). \tag{7}$$

After constituted by the above equation, eq. (2) becomes

$$[\rho c]_e\frac{\partial T}{\partial \tau} = \frac{\partial}{\partial x}\left(\lambda_e\frac{\partial T}{\partial x}\right) + q, \tag{8}$$

where

$$[\rho c]_e = \rho c + \varepsilon(1-S)\frac{d\rho_v}{dT}\cdot\Delta H, \tag{9}$$

$$\lambda_e = \lambda + \Delta H\cdot K_S. \tag{10}$$

Then from eqs. (3), (7) and (8), the following can be obtained:

$$-u_m\frac{\partial S}{\partial \tau} = -\frac{\partial}{\partial x}\left(K_S\frac{\partial T}{\partial x}\right) + f_T\frac{\partial}{\partial x}\left(\lambda_e\frac{\partial T}{\partial x}\right) + f_T q, \tag{11}$$

where

$$f_T = \frac{\varepsilon(1-S)}{[\rho c]_e}\cdot\frac{d\rho_v}{dT}. \tag{12}$$

Equations (8) and (11) are the heat and mass transfer equations for sublimation-condensation region.

1.2 Dried region

If the effects of temperature in the dried region on mass transport and those of vapor convection on heat transfer are neglected, the heat and mass transfer equations in the dried region are:

Mass balance equation

$$\varepsilon \frac{\partial \rho_v}{\partial \tau} = \frac{\partial}{\partial x}\left(D_e \frac{\partial \rho_v}{\partial x}\right); \tag{13}$$

energy balance equation

$$\rho c \frac{\partial T}{\partial \tau} = \lambda \frac{\partial^2 T}{\partial x^2} + q. \tag{14}$$

1.3 Sublimation front

If the vapor flow sublimated at the sublimation front is determined as

$$J_F = \left(-u_m S \frac{dX}{d\tau}\right)\bigg|_{x=X^-}, \tag{15}$$

the mass conservation equation for the front is

$$\left(-D_e \frac{\partial \rho_v}{\partial x}\right)\bigg|_{x=X^+} - \left(-K_S \frac{\partial T}{\partial x}\right)\bigg|_{x=X^-} = J_F, \tag{16}$$

and the energy balance equation is

$$\left(-\lambda_e \frac{\partial T}{\partial x}\right)\bigg|_{x=X^-} - \left(-\lambda \frac{\partial T}{\partial x}\right)\bigg|_{x=X^+} = J_F \cdot \Delta H. \tag{17}$$

2 Transport properties in sublimation-condensation region

The transport properties in the sublimation-condensation region are analyzed for frozen beef in this study and the basic physical properties in analysis are obtained from reference [10].

2.1 Effective diffusivity

The vapor flow in the sublimation-condensation region caused by the gradients of gas pressure and vapor concentration can be considered as the temperature effect and the vapor transport capacity by temperature gradient is symbolized by K_S. Considering that $K_r = 1 - S$, K_S should be the functions of temperature and saturation according to eq. (6). In addition, applying the transport properties of freeze-dried beef by Harper[9] and the expression $\rho_v = \rho_v(T)$ regressed from saturated vapor pressure data of ice, the variation of K_S with saturation at different temperatures can be illustrated (fig. 2). It shows that K_S is a linear function of saturation with decreasing tendency, which indicates that the vapor transport phenomenon is more obvious for smaller saturation conditions. It can also be seen that K_S becomes greater with temperature rising and so does its changing rate. In the case that $S=1$, $K_S=0$ is available for any temperature and the sublimation-condensation region disappears. Then sublimation takes place only at the sublimation front and the sublimation-condensation model turns into

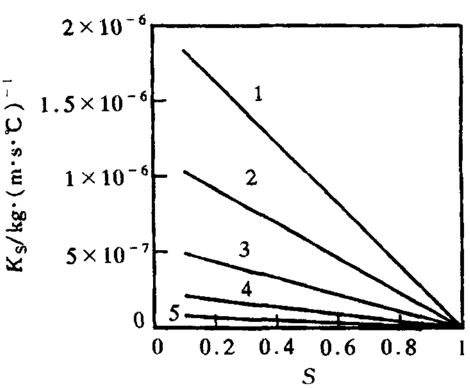

Fig. 2. Variation of K_S with S at different T. T/℃: 1, −1; 2, −10; 3, −20; 4, −30; 5, −40.

the sublimation interface model.

2.2 Effective thermal conductivity

Besides heat conduction of the material, phase change will cause heat transfer in the sublimation-condensation region which can also be described as the contribution of temperature gradient. In eq. (9) both contributions are included in the expression of effective thermal conductivity λ_e. If the true thermal conductivity λ is got by the volume average method, the variation of λ_e with T at different saturations can be shown (fig. 3). It can be seen that λ_e will increase with T rising and the increasing rate of λ_e will increase for smaller S. The figure also shows that λ_e becomes greater for larger S as $T < -19.3$℃ while for smaller S as $T > -19.3$℃. It should be noted that λ_e turns into a constant for any saturation as $T = -19.3$℃. This means that heat conduction of the material is the major mechanism of heat transfer in the sublimation-condensation region as $T < -19.3$℃ while phase change is the major mechanism as $T > -19.3$℃. The reason can be expressed as that for lower temperatures K_S is smaller and vapor transport in sublimation-condensation region is not so apparent that the role of heat conduction of the material becomes more significant and thus λ_e gets greater with S increasing. With regard to higher temperatures, the vapor transport capacity in the sublimation-condensation region rises and the effect of phase change on heat transfer increases as well so that λ_e increases with S decreasing. Moreover, both contributions of heat conduction and phase change are approximately equal as $T = -19.3$℃ and then λ_e does not change with S. The calculation also shows that λ_e is not the function of T when $S = 1$.

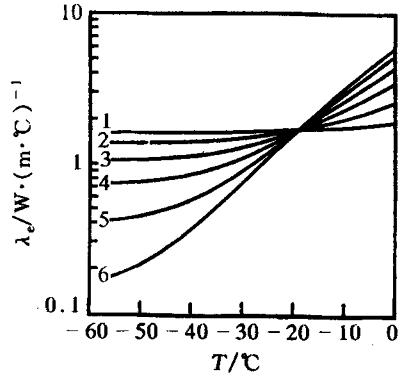

Fig. 3. Variation of λ_e with T at different S. S:1, 0.95; 2, 0.8; 3, 0.6; 4, 0.4; 5, 0.2; 6, 0.05.

These analyses prove that the transport properties of the material in the sublimation-condensation region change greatly with the variations of temperature and saturation so that the conclusion can be made that the present model is more available for practical operations than Luikov's model used by Fey and Boles[7]. In addition, the other coefficients in the present model are also studied by calculation. The results show that effective heat capacity $[\rho c]_e$ increases linearly with saturation rising and the effect of phase change can be neglected. On the other hand, eq. (11) indicates that the vapor sublimation can be created directed by internal heat source but the sublimation intensity depends on the power intensity of internal heat source.

3 Numerical simulation

The microwave freeze-drying process of the unsaturated frozen beef slab as illustrated in fig. 1 is simulated numerically and the difference from sublimation model is also discussed. In calculation, the boundary conditions and initial conditions are:

$$-\lambda_e \frac{\partial T}{\partial x}\bigg|_{x=0} = 0; \quad \left(-\lambda \frac{\partial T}{\partial x}\right)\bigg|_{x=l} = \alpha(T|_{x=l} - T_R); \quad \rho_v|_{x=l} = \frac{P_R}{RT|_{x=l}};$$

$$T|_{\tau=0} = T_0; \qquad S|_{\tau=0} = S_0; \qquad X|_{\tau=0} = l.$$

The electric field strength is considered homogeneous in calculation and the internal heat source intensity is expressed as[10]

$$q = kE^2,$$

where k is obtained by volume averaging from the data[10]1).

The operation conditions in the typical calculation are: $E = 135$ V/cm, $l = 0.008$ m, $P_R = 15$ Pa, $S_0 = 0.7$, $T_R = 20$℃, $T_0 = -15$℃.

The model is calculated by the variable time step finite difference method and the numerical error is controlled within 10^{-4}.

3.1 Distribution of temperature and saturation

Figure 4 shows the distribution profiles of temperature and saturation in the material during drying. The variation tendency of temperature is approximately like the results from sublimation interface model by Ma and Peltre[10] (fig. 4(a)). With the sublimation front shifting inside, the temperature there decreases rapidly, then increases slowly, and begins to decrease gradually near $X = 0.003$ m at last. This is caused by the effects of the variation of mass transfer resistance and heating power. The temperature curves slope gently in the sublimation-condensation region and the temperature decreases gradually from the center to the sublimation front while greater temperature gradients exist in the dried region, which is because of the great difference in the value of the effective thermal conductivity between the two regions.

Figure 4(b) indicates the profiles of saturation distribution in the material during drying. It shows that the saturation keeps unchanged in the sublimation-condensation region during the initial drying period. As $X = 0.007$ m, it begins to decrease obviously and the maximum change occurs in the material center. At the end of drying, the saturation has changed from 0.7 to 0.33. This proves that the sublimation-condensation region should not be neglected during microwave freeze-drying of unsaturated porous media.

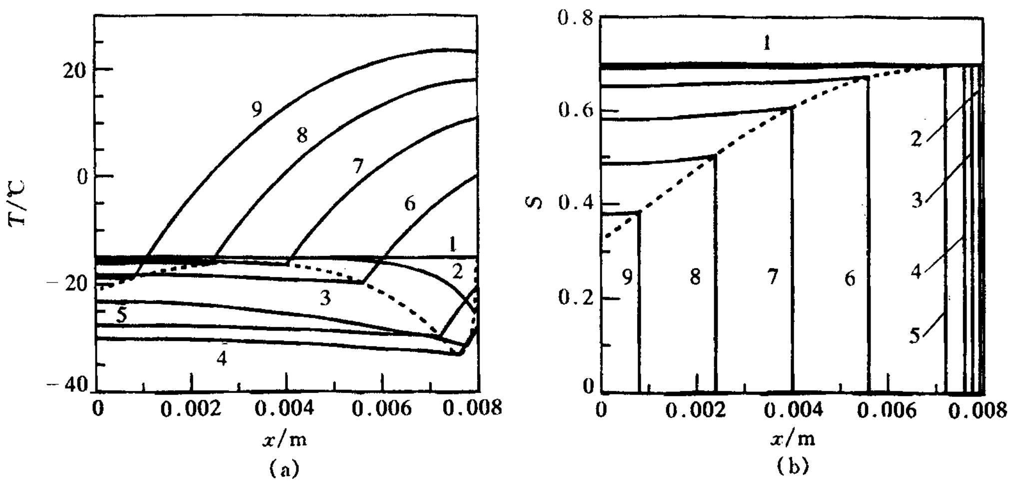

Fig. 4. Temperature and saturation distributions in drying. τ/s: 1, 0; 2, 0.1; 3, 3; 4, 99; 5, 530; 6, 2 218; 7, 3 592; 8, 5 926; 9, 8 184; – – –, sublimation front.

3.2 Drying rate

It can be seen from fig. 1 that the drying rate $J_v|_{x=X^+}$ consists of two vapor flows. One is

1) Wang Zhaohui, Heat and mass transfer during microwave freeze drying, *Ph.D. Thesis*, Nanjing: Southeast University, 1996.

$J_S|_{x=X^-}$ sublimated from the sublimation-condensation region and the other is J_F from the sublimation front. Fig. 5 shows the variations of $J_v|_{x=X^+}$ and $J_S|_{x=X^-}$ at different positions of the sublimation front. Obviously, the difference between the two flows is J_F. The figure indicates that both $J_v|_{x=X^+}$ and $J_S|_{x=X^-}$ are great as the sublimation front is near the surface. The former is because of the small resistance and large potential for mass transfer while the latter is due to the greater temperature difference between the material surface and the sublimation front resulting from the rapid decrease of the sublimation front temperature at the beginning of drying as illustrated by curves 2 and 3 in fig. 4(a). Then more vapor will flow from sublimation-condensation region as expressed by equation (5).

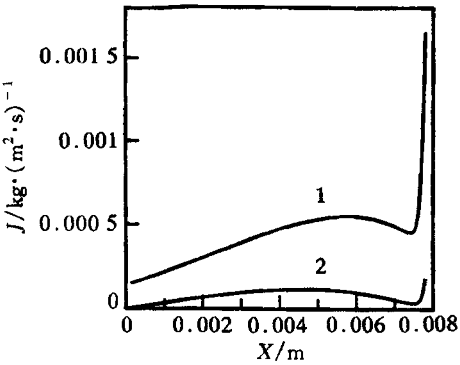

Fig. 5. Vapor flows at different sublimation front positions. 1, $J_v|_{x=X^-}$; 2, $J_S|_{x=X^+}$.

With the drying process propagating, both $J_v|_{x=X^+}$ and $J_S|_{x=X^-}$ decrease rapidly because the declining temperature of the material center as illustrated by curve 4 in fig. 4(a) decreases the mass transfer potentiality and the quick declining of average temperature of the sublimation-condensation region leads to the decrease of vapor transport capacity. As a result, $J_S|_{x=X^-}$ decreases sharply. Though $J_S|_{x=X^-}$ is great in the initial drying period, this period is so short that the saturation in the sublimation-condensation region does not change obviously. On the other hand, the increase of mass transfer resistance and the coupled effect with temperature make $J_v|_{x=X^+}$ decrease.

As the sublimation front shifts inside on, $J_v|_{x=X^+}$ and $J_S|_{x=X^-}$ reach their minimum values consequently and then begin to rise. Because of the larger increasing rate of $J_S|_{x=X^-}$, the saturation in the sublimation-condensation region decreases obviously as shown in fig. 4(b). As $X = 0.005\,8$ m, $J_v|_{x=X^+}$ reaches the maximum value and begins to decrease and so does $J_S|_{x=X^-}$ as $X = 0.004\,6$ m. All is caused by the distribution of temperature and saturation in the sublimation-condensation region and the complicated variations of temperature and saturation at the sublimation front.

The contribution of vapor from the sublimation-condensation region to the drying rate is different at different times. If $f_J = \dfrac{J_S|_{x=X^-}}{J_v|_{x=X^+}}$ is used to represent the contribution percentage of vapor from the sublimation-condensation region, the contribution from the sublimation front can be expressed as $1 - f_J$. Fig. 6 shows the variations of f_J at different sublimation front positions during drying. Therefore the contribution of the sublimation-condensation region to the drying rate is illustrated more clearly. It can be seen that the contribution experiences the processes of decreasing, increasing, and decreasing again. During these periods, the maximum f_J can reach 0.24 and the average value is about 0.15. It proves that the sublimation-

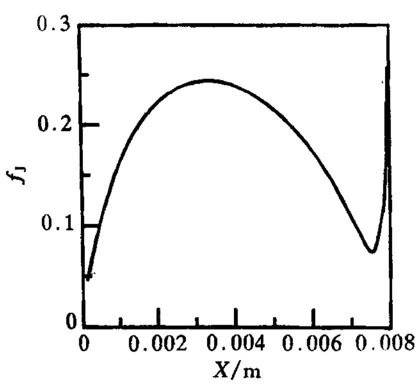

Fig. 6. Variation of f_J at different sublimation front positions.

condensation region plays an important role in microwave freeze-drying of unsaturated porous media.

3.3 Comparison with sublimation interface model

During microwave freeze-drying of unsaturated porous media, a great difference exists between the results considering and not considering the sublimation-condensation region due to the saturation variation in the sublimation-condensation region. In order to compare the two results, the sublimation interface model is calculated numerically under the same operation conditions. The numerical results show that as compared with the sublimation-condensation model, apparent difference exists in value though their temperature distribution shapes are similar. For example, the maximum extreme temperature of the sublimation interface in drying is -18.0℃ while that of the sublimation front is -15.9℃.

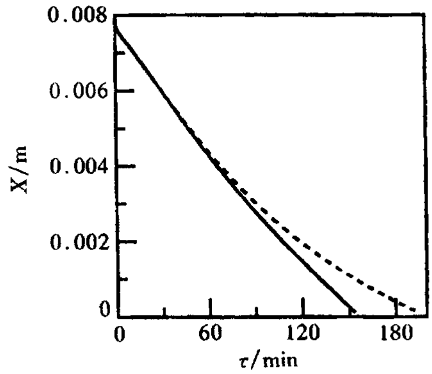

Fig. 7. X-τ curves of the two models. ——, Sublimation-condensation model; – – , sublimation interface model.

Figure 7 illustrates the position variations of the sublimation front or sublimation interface with time for the two models. It shows that both curves are overlapped in the beginning period. At about 60 min, the changing rate of the sublimation interface becomes smaller while that of the sublimation front keeps nearly constant. At the end of the drying process, it takes 200 min for the sublimation interface model while 150 min for the sublimation-condensation model, which is a great difference apparently.

Because of the saturation change in the sublimation-condensation region, the variation of the sublimation front does not represent the material mass loss in drying. Therefore the traditional method applying the variation curve of sublimation interface position as the drying curve[10] is not available here while

$$f_m = \int_0^X \frac{S}{S_0 l} \mathrm{d}x$$

indicates the moisture content fraction left in the material as $x = X$. The variation of f_m with time is just the drying curve for the sublimation-condensation model. Fig. 8 shows the drying curves of the sublimation-condensation model and the sublimation interface model under the same operation conditions. It can be seen that the disparity between these two curves is different from that in fig. 7 so that great error will be created to predict the material moisture loss with sublimation interface model.

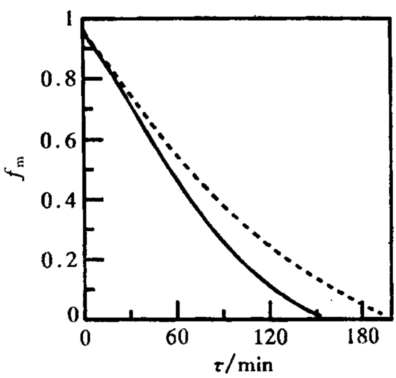

Fig. 8. Drying curves of the two models. ——, Sublimation-condensation model; – – –, sublimation interface model.

All the above indicates that the sublimation-condensation region affects significantly the microwave freeze-drying of unsaturated porous media and the sublimation-condensation model is more available for practical processes than the sublimation interface model.

4 Conclusions

A sublimation-condensation region exists during microwave freeze-drying of unsaturated porous media. The saturation in the sublimation-condensation region changes obviously during drying and its effect on heat and mass transfer is significant so that it should not be neglected. As compared with the sublimation interface model, which does not consider the sublimation-condensation region, the sublimation-condensation model is more available for practical drying processes. The analysis on transport properties in the sublimation-condensation region shows that the assumption of constant physical properties will deviate from the real case greatly.

References

1 Arsem, H. B., Ma, H. Y., Simulation of a combined microwave and radiant freeze dryer, *Drying Technology*, 1990, 8: 993.

2 Luikov, A. V., Systems of differential equations of heat and mass transfer in capillary-porous bodies (review), *Int. J. Heat Mass Transfer*, 1975, 18: 1.

3 Lin, S., An exact solution of the sublimation problem in a porous medium, *ASME J. Heat Transfer*, 1981, 103: 165.

4 Lin, S., An exact solution of the sublimation problem in a porous medium, Part II——with an unknown temperature and vapor concentration front, *ASME J. Heat Transfer*, 1982, 104: 808.

5 Fey, Y. C., Boles, M. A., An analytical study of the effect of the Darcy and Fick laws on the sublimation of a frozen semi-infinite porous medium, *ASME J. Heat Transfer*, 1987, 109: 1045.

6 Fey, Y. C., Boles, M. A., An analytical study of the effect of convection heat transfer on the sublimation of a frozen semi-infinite porous medium, *Int. J. Heat Mass Transfer*, 1987, 30: 771.

7 Fey, Y. C., Boles, M. A., An analytical study of vacuum-sublimation in an initially partially filled frozen porous medium with recondensation, *Int. J. Heat Mass Transfer*, 1988, 31: 1645.

8 Whitaker, S., Simultaneous heat, mass, and momentum transfer in porous media: A theory of drying, in *Advances in Heat Transfer*, Vol. 13, New York: Academic Press, 1977, 119—203.

9 Harper, J. C., Transport properties of gases in porous media at reduced pressures with reference to freeze drying, *AIChE J.*, 1962, 8: 298.

10 Ma, Y. H., Peltre, P., Freeze dehydration by microwave energy: Part I: Theoretical investigation, *AIChE J.*, 1975, 21: 335.